American Mineralogist, Volume 81, pages 1315–1320, 1996

Magnesium site exchange in forsterite: A direct measurement by high-temperature ^{25}Mg NMR spectroscopy

J.F. Stebbins

Department of Geological and Environmental Sciences, Stanford University, Stanford, California 94305, U.S.A.

Abstract

High-resolution ^{25}Mg NMR data are reported for a single crystal of pure forsterite (Mg_2SiO_4) at temperatures to about 1400 °C, which allow rates of exchange of Mg cations among specific sites in the structure to be obtained. Results are consistent with estimates of hopping frequencies derived from macroscopic diffusivity data, suggesting that this approach holds potential for tracing microscopic diffusion pathways in even very refractory minerals.

Introduction

Despite the large and increasingly precise data set on macroscopic rates of diffusion in silicates, very few direct observations of the atomic-scale details of diffusion pathways have been reported. Diffusion ultimately requires the motion of ions from one site to another, but in complex crystal structures there may be numerous "choices" as to which sites (occupied or vacant) are involved. Preferred diffusion pathways can be straight or tortuous, depending on the energetic costs of ion hopping among different sites. Long-range structural anisotropy may result in variation of bulk diffusivity with crystallographic orientation. Accurate models of diffusion, required for the extrapolation of laboratory data to geological time scales, thus require detailed microscopic information.

Recently we published high-resolution one-dimensional and two-dimensional ^6Li nuclear magnetic resonance (NMR) data on lithium orthosilicate (Li_4SiO_4) that showed exchange of Li^+ cations among sites with different numbers of first-neighbor O atoms (Stebbins et al. 1995b; Xu and Stebbins 1995). Exchange frequencies measured near ambient temperature accurately predicted Li^+ diffusivity as measured by electrical conductivity and produced the first direct information about relative exchange rates and energies for different sites. Here we extend this approach to the geologically more interesting (but experimentally much more challenging) problem of Mg^{2+} diffusion in olivine.

A variety of studies of cation diffusion in olivine have been conducted, motivated by the predominance of this phase in the upper mantle and its structural and compositional simplicity, and have been reviewed recently (Chakraborty et al. 1994). As in most oxides, bulk diffusion in olivine depends greatly on the concentration of defects, particularly M-site vacancies linked to the presence of Fe^{3+}. Local cation-hopping rates and directions must therefore also depend on concentration and location of defects. However, diffusive transport still requires the net motion of cations through the structure by exchange from one normally occupied site to another. In this study, we exploit the ability of high-resolution NMR spectroscopy to distinguish among different sites to monitor site-specific rates of cation exchange. For simplicity we began with an olivine that is nominally pure forsterite (Mg_2SiO_4).

In general, observation of useful ^{25}Mg NMR spectra in silicates is made difficult by the relatively low Larmor frequency ($<\frac{1}{3}$ that of ^{29}Si) and the relatively low isotopic abundance of this nuclide (10.1% of natural Mg). Second-order quadrupolar broadening is often large enough to make observation of useful magic-angle spinning (MAS) spectra of powdered samples difficult, although a few data have been reported (Dupree and Smith 1988; MacKenzie and Meinhold 1993, 1994a, 1994b; MacKenzie et al. 1993; Fiske and Stebbins 1994). However, this broadening is absent in static (non-MAS) single-crystal spectra, in which quadrupolar (and chemical-shift anisotropy) effects merely shift in frequency peaks that can be very narrow (and therefore readily observable). In materials in which other abundant, high Larmor frequency nuclides (e.g., ^{23}Na, ^{27}Al, ^{31}P) are absent or low in concentration, and the content of paramagnetic cations (e.g., Fe^{2+}) is low, line broadening caused by dipole-dipole coupling is also negligible. In such cases, ^{25}Mg single-crystal studies hold great promise.

One previous NMR study of ^{25}Mg in a single crystal of forsterite (Mg_2SiO_4) has been reported, in which the signal strength was greatly enhanced by the transfer of spin energy from unpaired electrons in Cr^{3+} dopant ions ("dynamic nuclear polarization," or DNP) at a temperature of 4.2 K (Derighetti et al. 1978). That study is a very useful starting point for interpretation of the results presented here, although the DNP technique would be difficult to apply at high temperature. To our knowledge, our results on forsterite are the first conventional NMR study of ^{25}Mg in a single-crystal oxide other than MgO (Stebbins 1995b).

0003–004X/96/1112–1315$05.00

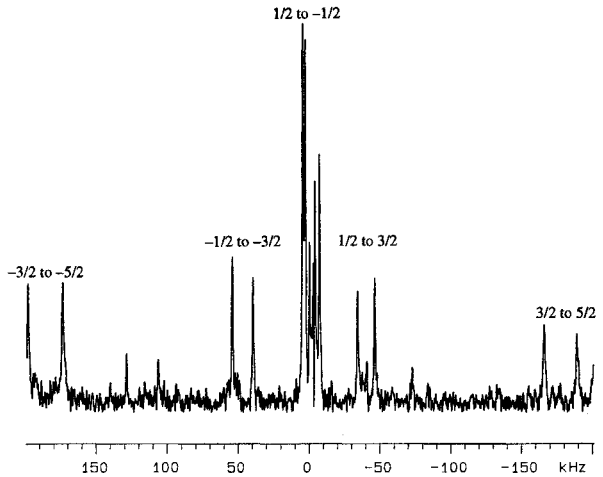

FIGURE 1. Single-crystal ^{25}Mg NMR spectrum of synthetic forsterite. In this orientation, satellite transitions are clearly visible for only the M2 peaks.

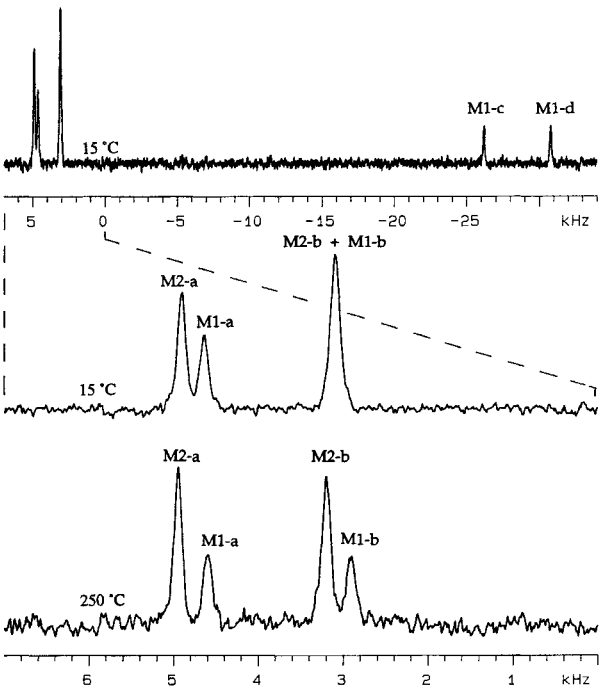

FIGURE 2. Spectra showing only central (½ to −½) transitions for a crystal fragment and orientation different from those shown in Figure 1. Note that at 15 °C, two peaks are coincident. This sample and orientation were used in the complete high-temperature study, as shown in Figure 4.

SAMPLES AND EXPERIMENTAL METHODS

NMR data were collected from two pieces of a single crystal of nominally pure forsterite (Mg_2SiO_4), synthesized by General Electric. Higher quality data were obtained from the larger sample, which measured about 7 × 7 × 10 mm. Analysis by glow-discharge mass spectrometry (Northern Analytical Laboratory) indicated that the material is extremely pure, with the only elements detectable at the 2–5 ppm level being Al (10 ppm) and Fe (5 ppm). H, N, and C were not analyzable by this method.

Spectra were obtained either with a Varian "wideline" probe with a horizontal solenoidal radio frequency (rf coil) (ambient temperature only) or with a resistively heated, home-built high-temperature probe. A modified Varian VXR-400S spectrometer was used, with a 9.4 T field providing a ^{25}Mg Larmor frequency of 24.5 MHz. All frequencies were referenced to a separate sample of 1 *M* aqueous $Mg(NO_3)_2$. For the larger forsterite sample, no sample container was used; the crystal was supported by the molybdenum-wire rf coil only. All experiments were performed in an atmosphere of N_2–3% H_2. Temperatures were calibrated in a separate experiment and are accurate to about ±10 °C. Frequency shifts caused by the heater current were negligible in comparison with those resulting from temperature effects on the structure. Spin-lattice relaxation times (T_1) were measured at several temperatures by the saturation-recovery method, and delay times between pulses were chosen to optimize signal-to-noise ratios. Single-pulse data acquisition was used throughout the study. Usable spectra could be obtained in a few hours at ambient temperature, but exchange broadening and other thermal effects required that the highest temperature spectra be collected in overnight experiments. The samples were oriented to within about 5° by single-crystal X-ray diffraction (XRD) after the NMR experiments. The high-temperature spectra discussed below were collected with the crystallographic *a* axis at approximately 90° to the external field $\mathbf{B}_0$ and the *c* axis at approximately 40° to $\mathbf{B}_0$.

RESULTS

Single-crystal spectra and peak assignments

As shown in Figure 1, the single-crystal ^{25}Mg peaks are quite narrow (about 100 Hz) at ambient temperature because of the lack of any significant disorder or nuclear or electronic dipolar broadening.

In some orientations, the quadrupolar satellite transitions could be easily observed with the high-power wideline probe. Both the central (½ to −½) and satellite (±½ to ±3/2 and ±3/2 to ±5/2) transitions, for both the M1 and M2 sites, are split because there are multiple, crystallographically equivalent orientations of the electric-field–gradient (EFG) tensor for each site with respect to the external magnetic field, resulting in different second-order quadrupolar shifts in the corresponding resonant frequencies. In the orientation most thoroughly studied at high temperature (Fig. 2), the central transition signal from the M2 site was split into two peaks, whereas that from M1 was split into four, consistent with a previous single-crystal study (Derighetti et al. 1978) and with the more symmetrical point group of M2 (*m*) in comparison with M1 ($\bar{1}$). The sizes of the quadrupolar splittings are

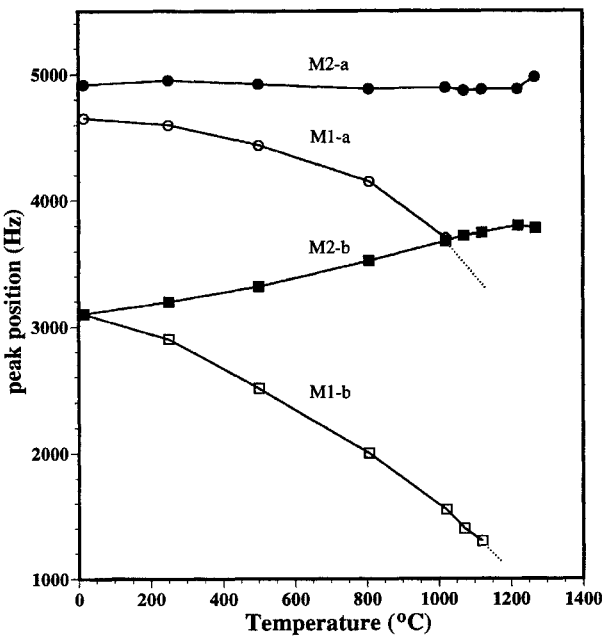

FIGURE 3. Peak positions as a function of temperature. Above 1000–1100 °C, the M1 peaks become too broad to observe readily. Uncertainties in both temperature and frequency are similar to or smaller than the symbol size.

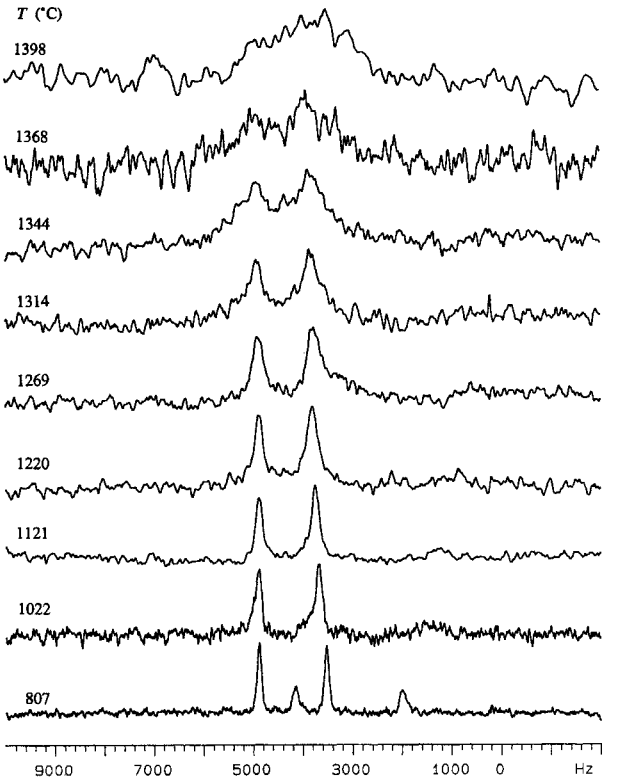

FIGURE 4. High-temperature spectra collected in situ at various temperatures. Note the broadening of the M1 peaks, followed by the broadening and merging of the M2 peaks caused by exchange averaging.

also consistent with the previous study, if adjusted for the difference in $\mathbf{B}_0$. At the eight-times higher field used in our experiments, chemical-shift anisotropy may also contribute to peak positions, but, given the known range of isotropic chemical shifts for ^{25}Mg [about 50 ppm (Fiske and Stebbins 1994)], this effect is probably limited to a few kilohertz. We arbitrarily labeled the split components "a", "b", etc., for convenience of discussion. Examination of the symmetry of the structure indicates that M1-a and M1-b are signals from sites related by the twofold screw axis parallel to *a* and thus are on adjacent octahedral chains. The M2-a and M2-b peaks are from sites related by the same symmetry element and thus represent adjacent, corner-shared octahedra.

Effects of temperature on peak positions

For the high-temperature studies, an orientation was chosen such that at ambient temperature the two M2 peaks and two of the four M1 peaks were close together, allowing high sensitivity to exchange averaging. With increasing temperature, the increased distortion of the sites shifted the M1 peaks to significantly lower frequency (greater second-order quadrupolar shift) (Fig. 3). Such a change is qualitatively consistent with the known increases in site distortion with increasing temperature (Hazen 1976). The orientation of the EFG for the M2 sites apparently leads, fortuitously, to relatively small temperature effects on positions of peaks for this site.

Effects of temperature on peak widths

As shown in Figures 4 and 5, the single, clearly observed M1 peak began to broaden substantially at about 1000 °C (M1-a happens to coincide with M2-b in this temperature range). The two M2 peaks began to broaden at about 1200 °C. At higher temperatures, the M1 peak became difficult to observe, and the M2 peaks eventually merged into a single broad peak. These changes in peak shape are of key importance for understanding cation dynamics.

Three possible mechanisms could contribute to peak broadening. It is conceivable, for example, that positional disorder increases with temperature to such an extent as to result in a wide range of M-site local geometries and, therefore, in a wide range of chemical or quadrupolar shift. There is no evidence from high-temperature XRD data to suggest that this is the case (Hazen 1976). Peak broadening could also result if spin-lattice relaxation becomes rapid with respect to the peak widths. This possibility was investigated by measuring T_1 at several temperatures. Although values dropped significantly from about 27 s at ambient temperature to about 0.2 s at 1268 °C, T_1 at all temperatures was at least two orders of magnitude greater than the inverse of the line widths (Fig. 5).

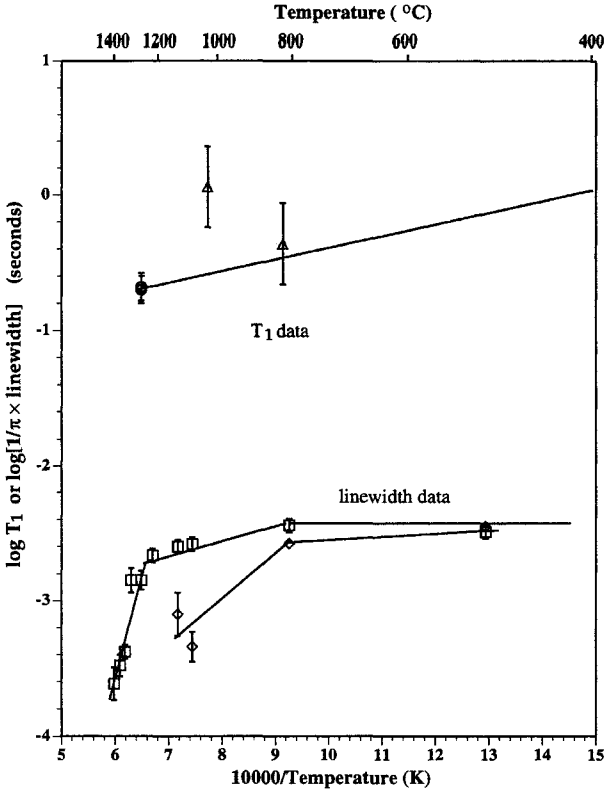

FIGURE 5. Peak width and spin-lattice relaxation time (T_1) data. Peak widths (lower data set) are plotted as $1/\pi \times$ line width, which would approach T_1 if the latter were responsible for peak broadening. Peak widths in this plot were approximated by fitting spectra with two peaks with unconstrained Gaussian/Lorentzian fractions for the M2 peaks. A single peak was fitted to M1. The solid line shown for the T_1 data (upper data set) is constrained by precise data at 15 °C (not shown, 27 ± 2 s). Solid lines show data trends only. Triangles = T_1 for small crystal; circles = T_1 for large crystal; squares = line widths for large crystal, average of M2-a and M2-b peaks; diamonds = line widths for M1-b peak.

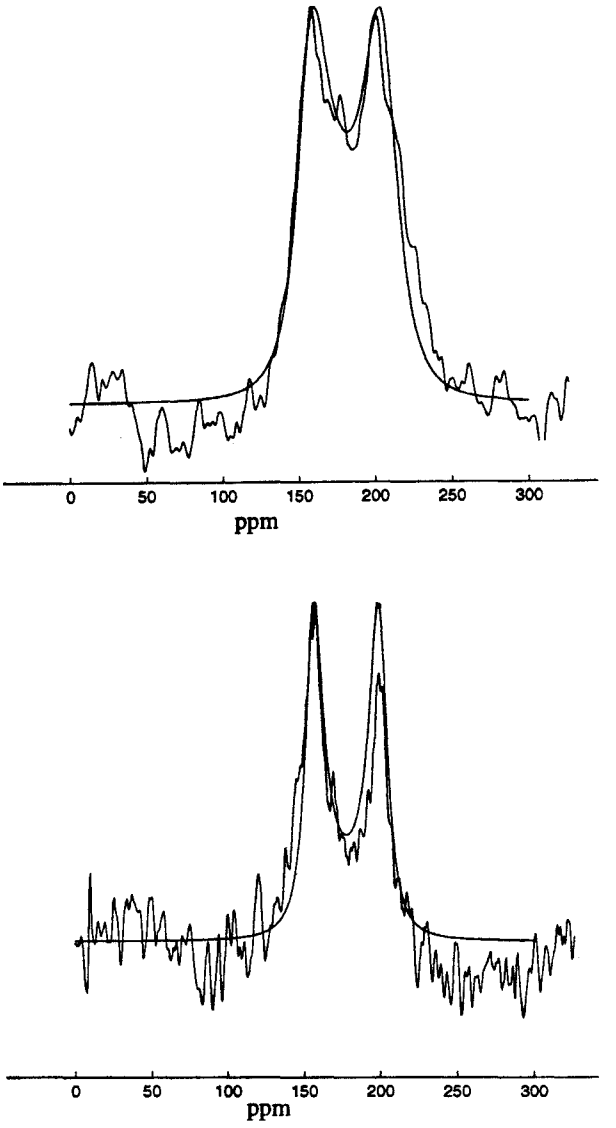

FIGURE 6. Simulations of two-site exchange for the M2 peaks. Upper spectrum = 1344 °C, 1800 Hz exchange frequency; lower spectrum = 1314 °C, 800 Hz. Solid lines are the best approximations to the overall experimental peak shapes. Note that scales are in parts per million and plot in the opposite direction from those in Figures 1, 2, and 4.

Thus, relaxation can also be discounted as a major cause of peak broadening.

The probable explanation for the broadening and partial merging of the peaks is exchange averaging. A well-known effect in NMR (and other spectroscopies), this process can be observed if the rate of exchange among distinct sites increases to a frequency similar to that of the separation in frequency of the corresponding peaks in the spectrum (Stebbins 1988, 1995a). As in earlier work on several silicate melts (Stebbins et al. 1995a), we used a simple two-site exchange model to simulate this process. Results of simulations (Fig. 6) give estimates of the exchange frequencies, which are best constrained between about 1300 and 1400 °C. At somewhat lower temperatures, the simulated values of the M2-M2 exchange frequency are probably maxima only, because some broadening is also apparently caused by M1-M2 exchange. The latter was simulated at 1121 °C only because of poor signal-to-noise ratios at other temperatures. Because some of the broadening of the M1 peaks could also have been caused by M1-M1 exchange, the latter estimate is particularly uncertain and remains to be investigated more precisely by future studies of other crystal orientations. Estimated exchange frequencies are shown in Figure 7.

DISCUSSION

Chakraborty et al. (1994) recently published data on Mg^{2+} tracer diffusion in two samples of nominally pure

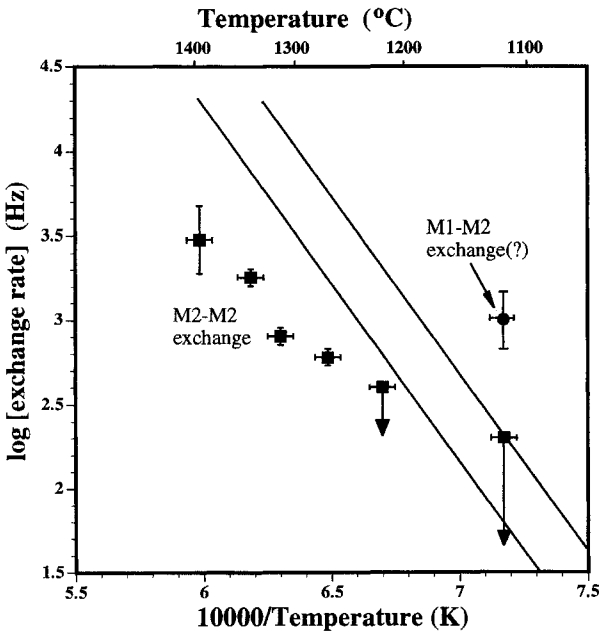

FIGURE 7. Cation-exchange rates based on line-shape simulations, in comparison with those predicted from the measured Mg-tracer diffusivity (Chakraborty et al. 1994). Approximations for three-dimensional (upper line) and one-dimensional (lower line) diffusion are shown. Points for M2-M2 exchange below about 1300 °C are probably estimates of maximum exchange frequency only, because significant peak broadening may be caused by M1-M2 exchange or possibly by slight positional disorder.

forsterite. Most data were collected for a sample with 120–180 ppm Fe (Fo-1), with the diffusion direction parallel to c; diffusion rates parallel to a or b are lower by factors of four to six but are less precisely known. The most complete data were reported for measurements made at low f_{O_2} (as in the present study), and no significant effects of H_2 or H_2O in the gas phase were noted. The diffusion coefficient D increased by about one log unit from an f_{O_2} of 10^{-12} to that of air, presumably because of an increase in the concentration of Fe^{3+}. A few data were collected at a single temperature for a sample with an Fe content of only 11 ppm (Fo-2). For this material, D was independent of f_{O_2} and was actually higher than for Fo-1 by about 0.5 log units at low f_{O_2}. For comparison with the NMR data on our Fe-poor sample, we therefore used the diffusion equation of Chakraborty et al. (1994) for forsterite Fo-1, adjusted it upward by 0.5 log unit, and assumed the activation energy to be independent of f_{O_2} over this interval.

The simplest model that relates cation site hopping to bulk diffusion is the Einstein-Smoluchovski equation, $D \approx d^2/A\tau$, where d is the jump distance, τ is the inverse of the jump frequency, and A is a geometric factor that is often considered to be six for three-dimensional diffusion and two for the one-dimensional case (such as diffusion along a chain). Shown in Figure 7 are exchange-rate ($1/\tau$) values estimated in this fashion from the data of Chakraborty et al. (1994), for both the three-dimensional and one-dimensional cases, assuming that diffusion along c is dominated by jumps along the M1 chains of approximately 0.30 nm, the typical M1-M1 distance. The one-dimensional case may be most appropriate because of the strong observed anisotropy.

Although the exchange frequencies most precisely measured by NMR are for M2-M2 exchange, they are close to those predicted from the diffusivity but are at a somewhat lower frequency. This difference is probably at least in part the result of a longer jump distance for M2-M2 exchange. For Mg exchange between corner-shared M2 sites (possibly by an adjacent edge-shared tetrahedral vacancy), the distance is about 0.38 nm. All else being equal, this should result in a reduction in hopping frequency by the square of the ratios of the distances, or about 0.21 log units. Hopping of Mg^{2+} cations from one M2 site to another along c, through the intervening octahedral vacancy, would not affect the NMR spectrum because such sites are magnetically equivalent in all orientations.

The preliminary data reported here demonstrate that site-specific exchange rates can be measured even in a material as refractory as forsterite and are reasonable in light of what is known about macroscopic diffusion. Future studies may be able to quantify rates for other sites, in particular the most critical M1-M1 rate, and the effects of f_{O2} and of impurity substituents.

ACKNOWLEDGMENTS

I thank Ian Carmichael for graciously supplying the forsterite sample, and Sumit Chakraborty for productive discussions about diffusion in olivine. Careful reviews from Brian Phillips, Christian Jäger, and Sumit Chakraborty improved the paper significantly. This study was funded by the National Science Foundation, EAR-9506393.

REFERENCES CITED

Chakraborty, S., Farver, J.R., Yund, R.A., and Rubie, D.C. (1994) Mg tracer diffusion in synthetic forsterite and San Carlos olivine as a function of P, T, and f_{O_2}. Physics and Chemistry of Minerals, 21, 489–500.

Derighetti, B., Hafner, S., Marxer, H., and Rager, H. (1978) NMR of ^{29}Si and ^{25}Mg in Mg_2SiO_4 with dynamic polarization technique. Physics Letters, 66, 150–152.

Dupree, R., and Smith, M.E. (1988) Solid-state magnesium NMR spectroscopy. Journal of the Chemical Society, Chemical Communications, 1483–1485.

Fiske, P.S., and Stebbins, J.F. (1994) The structural role of Mg in silicate liquids: A high-temperature ^{25}Mg, ^{23}Na, and ^{29}Si NMR study. American Mineralogist, 79, 848–861.

Hazen, R.M. (1976) Effects of temperature and pressure on the crystal structure of forsterite. American Mineralogist, 61, 1280–1293.

MacKenzie, K.J.D., and Meinhold, R.H. (1993) A ^{25}Mg magic-angle spinning nuclear magnetic resonance study of the thermal decomposition of magnesium carbonate. Journal of Materials Science Letters, 12, 1696–1698.

MacKenzie, K.J.D., Meinhold, R.H., Sherriff, B.L., and Xu, Z. (1993) ^{27}Al and ^{25}Mg solid-state magic-angle spinning nuclear magnetic resonance study of hydrotalcite and its thermal decomposition sequence. Journal of Materials Chemistry, 3, 1263–1269.

MacKenzie, K.J.D., and Meinhold, R.H. (1994a) ^{25}Mg nuclear magnetic resonance spectroscopy of minerals and related inorganics: A survey study. American Mineralogist, 79, 250–260.

———(1994b) The thermal reactions of synthetic hectorite studied by ^{29}Si, ^{25}Mg and ^{7}Li magic angle spinning nuclear magnetic resonance. Thermochimica Acta, 232, 85–94.

Stebbins, J.F. (1988) NMR spectroscopy and dynamic processes in mineralogy and geochemistry. In F.C. Hawthorne, Ed., Spectroscopic methods in mineralogy and geology, p. 405–430. Mineralogical Society of America, Washington, DC.

———(1995a) Dynamics and structure of silicate and oxide melts: Nuclear magnetic resonance studies. In J.F. Stebbins, P.F. McMillan, and D.B. Dingwell, Eds., Structure, dynamics, and properties of silicate melts, p. 191–246. Mineralogical Society of America Reviews in Mineralogy, Washington, DC.

———(1995b) Magnesium site exchange and diffusion in forsterite: Direct quantification using high temperature NMR. Eos, 76, 683.

Stebbins, J.F., Sen, S., and Farnan, I. (1995a) Silicate species exchange, viscosity, and crystallization in a low-silica melt: In situ high-temperature MAS NMR spectroscopy. American Mineralogist, 80, 861–864.

Stebbins, J.F., Xu, Z., and Vollath, D. (1995b) Cation exchange rate and mobility in aluminum-doped lithium orthosilicate: High-resolution lithium-6 NMR results. Solid State Ionics, 78, L1–L8.

Xu, Z., and Stebbins, J.F. (1995) Cation dynamics and diffusion in lithium orthosilicate: Two-dimensional lithium-6 NMR. Science, 270, 1332–1334.

MANUSCRIPT RECEIVED MARCH 18, 1996
MANUSCRIPT ACCEPTED JULY 25, 1996